Nonlinear Quantum Noise Dynamics in Ultrafast Nonlinear Nanophotonics

Edwin Ng[1,2,*], **Ryotatsu Yanagimoto**[2,*], **Marc Jankowski**[1,2], **and Hideo Mabuchi**[2]

[1] *Physics & Informatics Laboratories, NTT Research, Inc., Sunnyvale, California 94085, USA*
[2] *E. L. Ginzton Laboratory, Stanford University, Stanford, California 94305, USA*
[*] *These authors contributed equally to this work. Email: edwin.ng@ntt-research.com, ryotatsu@stanford.edu*

Abstract: We present a split-step framework for simulating nonlinear propagation of multimode quantum noise and entanglement in ultrafast pulses, beyond conventional linearized-noise approximations. We apply our method to model state-of-the-art dispersion-engineered devices on thin-film lithium niobate.

Traditionally, the high intensities required to trigger nonlinear optical phenomena have largely restricted the operation of nonlinear photonic devices to regimes in which the scale of quantum fluctuations are very small relative to the scale of the mean field (typically millions of photons or more). In these regimes—which include the generation of squeezed light or entangled photons in bulk or fiber nonlinear media—quantum fluctuations and their correlations (e.g., multimode entanglement) are conventionally treated as linear perturbations to the mean-field dynamics [1–3]. However, with the advent of dispersion-engineered waveguides on novel material platforms like thin-film lithium niobate (TFLN), the threshold for observing coherent nonlinear dynamics is rapidly approaching levels involving only dozens to hundreds of photons even in single-pass waveguides [4–6].

In approaching this "mesoscopic" regime of nonlinear optics, the interplay between quantum noise and the mean-field dynamics can become non-trivial, and in general, non-Gaussian features such as Wigner-function negativity emerge in the deeply quantum (i.e., "microscopic"), ultra-low-loss limit. But near the classical-quantum transition, especially with moderate amounts of loss, we expect Gaussian-state approximations [2] or mixtures thereof to provide relevant information about the nonlinear system dynamics, even when linearized approaches show significant discrepancies [4]; e.g., see Fig. 1(a). In fact, even in a non-Gaussian full-quantum theory, we expect such "nonlinear Gaussian models" to help facilitate efficient reduced quantum representations [4]. With this context, we present here a split-step, Gaussian-state framework for modeling pulse propagation that distinctively features *nonlinear noise dynamics* despite its Gaussian-state nature.

While our approach is general, we focus here on $\chi^{(2)}$ pulse propagation under a co-propagating Hamiltonian

$$\frac{\mathrm{i}\hbar}{2}\int \mathrm{d}z\, \varepsilon\big(\hat{\psi}_z\hat{\phi}_z^{\dagger 2} - \hat{\psi}_z^\dagger\hat{\phi}_z^2\big) + \hbar\int\frac{\mathrm{d}k}{2\pi}\Big(\Omega_1(k)\hat{\Phi}_k^\dagger\hat{\Phi}_k + \Omega_2(k)\hat{\Psi}_k^\dagger\hat{\Psi}_k\Big) \tag{1}$$

where $\hat{\phi}_z$ and $\hat{\psi}_z$ are, respectively, the fundamental-harmonic (FH) and second-harmonic (SH) annihilation operators at pulse-envelope coordinate z, obeying $\big[\hat{\psi}_z, \hat{\psi}_{z'}^\dagger\big] = \big[\hat{\phi}_z, \hat{\phi}_{z'}^\dagger\big] = \delta(z-z')$ and $\big[\hat{\phi}_z, \hat{\psi}_{z'}^\dagger\big] = 0$, and we define corresponding wavespace operators as $\hat{\Phi}_k := \int \mathrm{e}^{-\mathrm{i}kz}\,\hat{\phi}_z\,\mathrm{d}z$ (and similarly for $\hat{\Psi}_k$). This Hamiltonian generates propagation along time coordinate t, which can be expressed as quantized coupled-wave equations (CWEs)

$$\partial_t\hat{\phi}_z = \varepsilon\hat{\psi}_z\hat{\phi}_z^\dagger - \mathrm{i}\Omega_1(-\mathrm{i}\partial_z)\hat{\phi}_z, \qquad \text{and} \qquad \partial_t\hat{\psi}_z = -\frac{\varepsilon}{2}\hat{\phi}_z^2 - \mathrm{i}\Omega_2(-\mathrm{i}\partial_z)\hat{\psi}_z. \tag{2}$$

The first and second terms of the Hamiltonian (and the CWEs) describe the nonlinear and linear (dispersive) parts of the evolution, respectively, and they do not commute in general. Classically, similar CWEs can be efficiently solved using Fourier split-step methods, and the same can be done for the quantized theory, *provided* we can efficiently compute the two differential steps. The linear dispersive step is trivial under a split-step formulation, so we focus only on the nonlinear (first) terms in (2), which we denote with the shorthands $\dot{\mathcal{N}}\hat{\phi}_z$ and $\dot{\mathcal{N}}\hat{\psi}_z$, respectively.

Our central interest is the evolution of the *quantum fluctuations* $\delta\hat{\phi}_z := \hat{\phi}_z - \langle\hat{\phi}_z\rangle$ and $\delta\hat{\psi}_z := \hat{\psi}_z - \langle\hat{\psi}_z\rangle$. In a conventional *linearized approach* to quantum noise [1], we first assume the mean fields obey the *classical* CWEs

$$\dot{\mathcal{N}}\langle\hat{\phi}_z\rangle \approx \varepsilon\langle\hat{\psi}_z\rangle\langle\hat{\phi}_z^\dagger\rangle, \qquad \text{and} \qquad \dot{\mathcal{N}}\langle\hat{\psi}_z\rangle \approx -\frac{\varepsilon}{2}\langle\hat{\phi}_z\rangle^2, \tag{3}$$

which are solved, e.g., with a classical split-step method. An additional linearized approximation then gives

$$\dot{\mathcal{N}}\delta\hat{\phi}_z \approx \dot{\mathcal{N}}\hat{\phi}_z - \dot{\mathcal{N}}\langle\hat{\phi}_z\rangle \approx \varepsilon\big(\langle\hat{\psi}_z\rangle\delta\hat{\phi}_z^\dagger + \langle\hat{\phi}_z^\dagger\rangle\delta\hat{\psi}_z\big), \qquad \text{and} \qquad \dot{\mathcal{N}}\delta\hat{\psi}_z \approx \dot{\mathcal{N}}\hat{\psi}_z - \dot{\mathcal{N}}\langle\hat{\psi}_z\rangle \approx -\varepsilon\langle\hat{\phi}_z\rangle\delta\hat{\phi}_z. \tag{4}$$

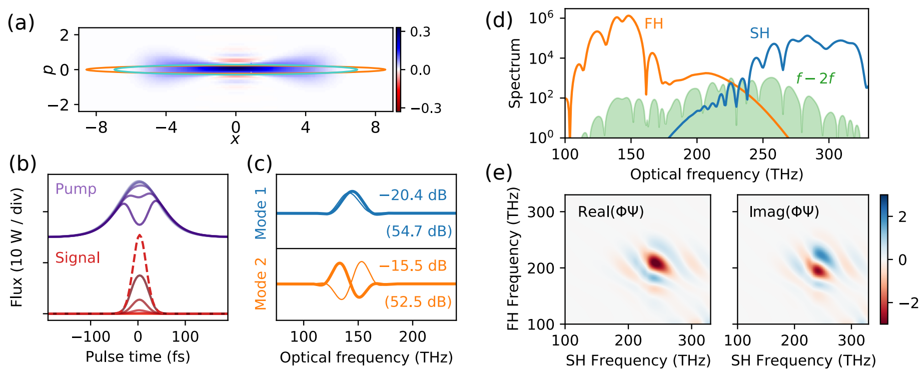

Fig. 1. (a) Linearized (orange) vs nonlinear (cyan) Gaussian approximations to a *non-Gaussian* state. (b) Parametric florescence dynamics in a TFLN waveguide (Model 1; see Ref. [5]), showing pump depletion and deviations from linearized predictions (dashed). (c) Two most major squeezing supermodes [1] produced by Model 1 (real vs imag parts: thick vs thin lines; antisqueezing in parentheses). (d) Supercontinuum generation in a TFLN waveguide (Model 2; see Ref. [6]), including beat note spectrum. (e) Covariances $\langle \delta\hat{\Phi}_k \delta\hat{\Psi}_{k'} \rangle$ (arb. units) between FH and SH spectral components produced by Model 2. We assume FH losses of $\sim 30\,\mathrm{dB/m}$ throughout.

Because these equations of motion are linear, they can be straightforwardly solved *assuming* the solution to (3). It is worth noting there is conceptual inconsistency in the linearized approach, as the mean-field dynamics (3) assume the field is in a coherent state, while (4) can in general produce, e.g., multimode squeezed states.

In mesoscopic regimes, however, nonlinear interactions may become strong enough for this separation of scales to fail. To address this issue, we turn to a more systematic approximation in which we assume the system is in an arbitrary multimode *Gaussian state* [2], in which we still assume all operator correlations can be reduced to means and covariances, but we *do not* assume linear fluctuation dynamics. In this case, we have, without approximations,

$$\dot{\mathcal{N}}\langle\hat{\phi}_z\rangle = \varepsilon\big(\langle\hat{\psi}_z\rangle\langle\hat{\phi}_z^\dagger\rangle + \langle\delta\hat{\phi}_z^\dagger\delta\hat{\psi}_z\rangle\big), \qquad \text{and} \qquad \dot{\mathcal{N}}\langle\hat{\psi}_z\rangle = -\frac{\varepsilon}{2}\big(\langle\hat{\phi}_z\rangle^2 + \langle\delta\hat{\phi}_z^2\rangle\big), \tag{5}$$

while for the covariances, we have in general six equations of motion. For the terms directly appearing in (5),

$$\varepsilon^{-1}\dot{\mathcal{N}}\langle\delta\hat{\phi}_z\delta\hat{\phi}_{z'}\rangle \approx \langle\hat{\psi}_z\rangle\langle\delta\hat{\phi}_z^\dagger\delta\hat{\phi}_{z'}\rangle + \langle\hat{\psi}_{z'}\rangle\langle\delta\hat{\phi}_z\delta\hat{\phi}_{z'}^\dagger\rangle + \langle\hat{\phi}_z^\dagger\rangle\langle\delta\hat{\phi}_{z'}\delta\hat{\psi}_z\rangle + \langle\hat{\phi}_{z'}^\dagger\rangle\langle\delta\hat{\phi}_z\delta\hat{\psi}_{z'}\rangle, \tag{6a}$$

$$\varepsilon^{-1}\dot{\mathcal{N}}\langle\delta\hat{\phi}_z^\dagger\delta\hat{\psi}_{z'}\rangle \approx -\langle\hat{\phi}_{z'}\rangle\langle\delta\hat{\phi}_z^\dagger\delta\hat{\phi}_{z'}\rangle + \langle\hat{\psi}_z^\dagger\rangle\langle\delta\hat{\phi}_z\delta\hat{\psi}_{z'}\rangle + \langle\hat{\phi}_z\rangle\langle\delta\hat{\psi}_z^\dagger\delta\hat{\psi}_{z'}\rangle, \tag{6b}$$

where the *only* approximations made above are that third-order central moments of the form $\langle\delta\hat{a}\,\delta\hat{b}\,\delta\hat{c}\rangle = 0$, which is true for all Gaussian states. Similar equations can be obtained for the four other covariances $\langle\delta\hat{\phi}_z^\dagger\delta\hat{\phi}_{z'}\rangle$, $\langle\delta\hat{\phi}_z\delta\hat{\psi}_{z'}\rangle$, $\langle\delta\hat{\psi}_z\delta\hat{\psi}_{z'}\rangle$, and $\langle\delta\hat{\psi}_z^\dagger\delta\hat{\psi}_{z'}\rangle$. It is worth noting that (5) and (6) are *coupled, nonlinear* equations of motion, where the means drive the evolution of the covariances, but also vice versa. Numerically, they are efficient to solve using Fourier split-step methods, only requiring $\mathcal{O}(N^2\log N)$ cost for N simulation bins.

A particularly striking example of nonlinear quantum noise dynamics is the *depletion* of an SH pump via intense parametric fluorescence in FH, violating undepleted-pump (linearized) approximations conventionally employed to analyze squeezing [3]. Using similar parameters to recent demonstrations [5] of ultrabroadband parametric amplification in dispersion-engineered TFLN, Fig. 1(b) shows that our model successfully captures this pump depletion effect. Furthermore, with access to the complete covariance matrices $\langle\delta\hat{\phi}_z\delta\hat{\phi}_{z'}\rangle$ and $\langle\delta\hat{\phi}_z^\dagger\delta\hat{\phi}_{z'}\rangle$, we can calculate squeezing supermodes as shown in Fig. 1(c), which can aid in the design of ultrabroadband TFLN-based squeezers; compared to semiclassical Monte-Carlo simulations [5], our approach requires integrating only one trajectory (of $\mathcal{O}(N^2)$ variables). Finally, to demonstrate the versatility of our method, we also show in Fig. 1(d,e) simulations of $\chi^{(2)}$ supercontinuum generation based on ultrabroadband second-harmonic generation [6]; such results may be useful, e.g., in exploring the quantum-noise limits of TFLN-based devices for $f-2f$ detection.

References

1. H. A. Haus and Y. Lai, J. Opt. Soc. Am. B **7**, 386 (1990); A. Hosaka et al., Phys. Rev. A **94**, 053833 (2016); M. Kizmann et al., Nat. Phys. **15**, 960 (2019); L. G. Helt and N. Quesada, J. Phys. Photon. **2**, 035001 (2020).
2. S. Olivares, Eur. Phys. J. Spec. Top. **203**, 3 (2012); S. L. Braunstein and P. van Loock, Rev. Mod. Phys. **77**, 513 (2005).
3. W. Wasilewski et al., Phys. Rev. A **73**, 063819 (2006); A. Christ et al., New. J. Phys. **13**, 033027 (2011).
4. R. Yanagimoto, E. Ng et al., arXiv:2111.13799 [quant-ph]
5. M. Jankowski, N. Jornod et al., arXiv:2104.07928 [physics.optics]; L. Ledzema, R. Sekine, Q. Guo et al., arXiv:2104.08262 [physics.optics]; M. Jankowski et al., J. Phys. Photonics **3**, 042005 (2021).
6. M. Jankowski et al., arXiv:2102.12856 [physics.optics]